Desalination and Water Treatment
www.deswater.com

doi:10.5004/dwt.2018.23240

135 (2018) 108–123
December

Application of transcritical CO_2 in multi-effect desalination system: energetic and exergetic assessment and performance optimization

Aida Farsi[a], Mehran Ameri[b,*], S.M. Hojjat Mohammadi[a]

[a]*Department of Energy, Institute of Science and High Technology and Environmental Sciences, Graduate University of Advanced Technology, Kerman, Iran, email: aidafarsi@yahoo.com (A. Farsi), smh.mohammadi@kgut.ac.ir (S.M. Hojjat Mohammadi)*
[b]*Department of Mechanical Engineering, Shahid Bahonar University of Kerman, Kerman, Iran, Tel. 983412111763, Fax 98 3412120964, email: ameri_mm@uk.ac.ir (M. Ameri)*

Received 7 January 2018; Accepted 3 October 2018

ABSTRACT

A model of cogeneration system based on low temperature refrigeration and water desalination is proposed. The cooling side is CO_2 transcritical refrigeration, and the water purification side is multi-effect desalination (MED). The MED subsystem can either be Boosted-MED or MED-pre-heaters (PHs) with a sensible heat source of transcriticalCO_2 leaving the compressor. A thermodynamic model was presented to reveal the effects of key operating parameters on the system's performances. Since the two products of these combined systems (cooling demand and fresh water) have different real thermodynamic value and the variation of COP and recovery ratio are in a contrary way, the exergetic analysis has been conducted to reveal the optimum performance condition using Genetic Algorithm as a powerful tool. The optimum design led to the selection of a MED-CO_2 Refrigeration system with the highest exergy efficiency. The variation of exergy destruction in each system component has also been investigated to clarify the exergy efficiency trend. Results show that the exergy efficiency is highly affected by COP rather than recovery ratio; with an increase in the compressor outlet pressure after the optimum point, COP reduces slightly but the recovery ratio increases sharply. So, the exergy efficiency has no considerable reduction after its maximum point. Furthermore, by reducing in TBT, the exergy destruction of the whole replaced system decreases steadily leads to the consistent rise in the exergy efficiency. Finally, in order to define the effects of the operating parameters on the system performance, a sensitivity analysis is conducted. From the results, the compressor outlet pressure has the most influence on the COP and second law efficiency with the highest sensitivity value,while for the recovery ratio, the ambient temperature is the most effective parameter.

Keywords: Tanscritical carbon dioxiderefrigeration; MED; Energetic and exergetic analysis; Genetic algorithm optimization; Sensitive analysis

1. Introduction

Healthy water crisis and the increasing demand of cooling are two important and critical problems for most countries, especially in tropic areas. Although, the need for these two products usually coincides, in many regions, they are produced separately by consuming significant energy.

1.1. Water desalination systems

The traditional methods that are widely used for water desalination are reverse osmosis, membrane separation and thermal desalination. In thermal desalination, salt is removed from sea water by evaporation and then condensation. In reverse osmosis technique, salt is removed by crossing sea water through some semipermeable membranes. In this method, a high pressure difference is needed between two sides of membranes. This high pressure difference can be supplied by a considerable electrical energy consumption. Membrane method has been known

*Corresponding author.

for its high recovery and low energy consumption [1]. Although thermal desalination methods consume more energy compared to membrane type, they have remained the most common desalination technology. This is mainly because of no need to discharge brine chemicals into the sea. It is also suitable to use industrial plants waste heat recovered to run thermal desalination systems. Among different thermal desalination systems, MED has been more attractive than multi-stage-flash (MSF); due to less power consumption, lower corrosion rate and lower desalted water costs [1]. It is a well-founded desalination technology that recycles the enthalpy of vaporization in successive stages to achieve a high gained output ratio (GOR). Its reliability and robustness to fouling make it a fascinating choice for water treatment plants [2]. MSF, MED and mechanical vapor compression (MVC) are appropriate for 100–500,000 m^3/d fresh water production capacity plant. The typical specific energy consumption of MSF and MED differs from 150 to 300 kJ/kg, with additional electrical power input of 2–4 kWh/m^3 for pumping seawater. On the other hand, for MVC the energy consumption is about 8–15 kWh/m^3 [3]. Samake et al. [4] performed a parametric study of MED system combined with a thermal vapor compression (TVC) and investigated the effects of design variables based on the first and second laws of thermodynamic on the operating quantities and performance of the system. Gude and Nirmalakhandan [5] offered an MED combined with an absorptionheat pump (ABHP) in which the rejected absorption heat is the energy source of MED water treatment system.

Conventional MED uses the latent heat of steam condensation as heat source. It fails to use the potential of sensible heat source which is a restriction of its inherent design. On the other hand, the sensible heat sources such as waste heat and renewable energies, require specific approaches to open their potential and they are the promising resources for water desalination process. Farsi et al. [6] proposed new combination of CO_2 transcritical refrigeration and MED. They declared that using supercritical CO_2 as a novel heat source presents a better heat transfer process compared to the steam driven MED. Christ et al. [7,8] discussed a new model of water treatment systems named as Boosted-MEDs which are able to run by sensible heat sources. They conducted a comparison between the proposed system with pre-heaters (PHs) and the simple parallel MED. Results indicated that for the input temperature of 80°C, the boosted model can produce 20% more pure water, compared to simple MED and pre-heaters. Dincer et al. [9] proposed a thermodynamic model for the combination of micro gas turbine cycle and solid oxide fuel-cell with MED equipped with thermal vapor compression. They showed that the pressure of fuel cell stack has a considerable effect on the power system and pure water production capacity.

1.2. Supercritical CO_2 refrigeration systems

In recent years, transcritical carbon dioxide refrigeration systems have been considerably noticed. Unlike synthetic refrigerants (HCFCs) that have adverse effects on ozone layer and weather conditions, use of a nonflammable, nontoxic and eco-friendly refrigerant; CO_2, has been developed and commercialized. Therefore, utilization of CO_2 in refrigeration cycles reduces environmental impacts. These systems can refrigerate the area until –40°C [10]. Since the supercritical CO_2 refrigeration cycle operates in high pressure levels, the rejected heat and dissipative exergy from its gas-cooler is considerable.

Several analyzes and studies have been carried out in order to improve the performance of CO_2 refrigeration systems. While, others studied the combination of CO_2 refrigeration systems with different plants in order to introduce multi-generation systems. Sarkar and Agrawal [12] tested a two-stage compression super-critical CO_2 cycle with an economizer. They claimed that the cooling COP enhanced by 47.3% over a basic conventional super-critical system. Yang et al. [13] concluded that the use of an expander instead of an expansion valve presented 50% decrease in the exergy loss resulting in 30% improvement in the system exergy efficiency. Shariatzadeh et al. [14] have compared four different configurations of CO_2 refrigeration system from the aspect of coefficient of performance (COP) and exergy. They showed that the system with expander and without internal heat-exchanger has the highest COP, minimum total exergy distruction and maximum exergy efficiency. Wang et al. [15] have suggested a system which can produce cooling, heating and power in the same time, using Brayton and supercritical CO_2 refrigeration cycles simultaneously. In their study, a mathematical model is used for simulation, energy and exergy analysis of the proposed tri-generation system.

Since, the combination of MED system and transcritical CO_2 refrigeration is proposed by Farsi et al. [6] and they studied the heat transfer aspect of this system, it would be necessary to investigate the thermodynamic operation of system. So in this paper, a thermodynamic simulation including the detailed energy and exergy model is performed. The influence of operating conditions such as; evaporator temperature, ambient temperature, compressor outlet pressure and first effect brine temperature (TBT) on the COP and the produced desalted-water flow rate are investigated. Furthermore, the second law of thermodynamics specifies the path in which the efforts of engineering should be focused by determining the sources of losses to promote the operation of a system [16]. Accordingly, in exergy analysis, the dissipated exergy in each system component and the changes of exergy destruction in different operating conditions has been surveyed and calculated. The primary objective of this research is to study the performance of the hybrid system, using energy and exergy analysis methods. A further objective is to model the system components via exergy balance equations in order to discover the main sources of losses to enhance the system performance. Finally in the sensitive analysis, the influence of operating parameters on the system responses value, including COP, recovery ratio and second law efficiency is conducted to determine the most effective parameter.

2. Description and modeling

2.1. The combined system description

Fig.1 shows a schematic diagram of the Boosted-MED-CO_2 refrigeration system. The supercritical CO_2 is a sensible heat source of the MED system [6]. Since CO_2

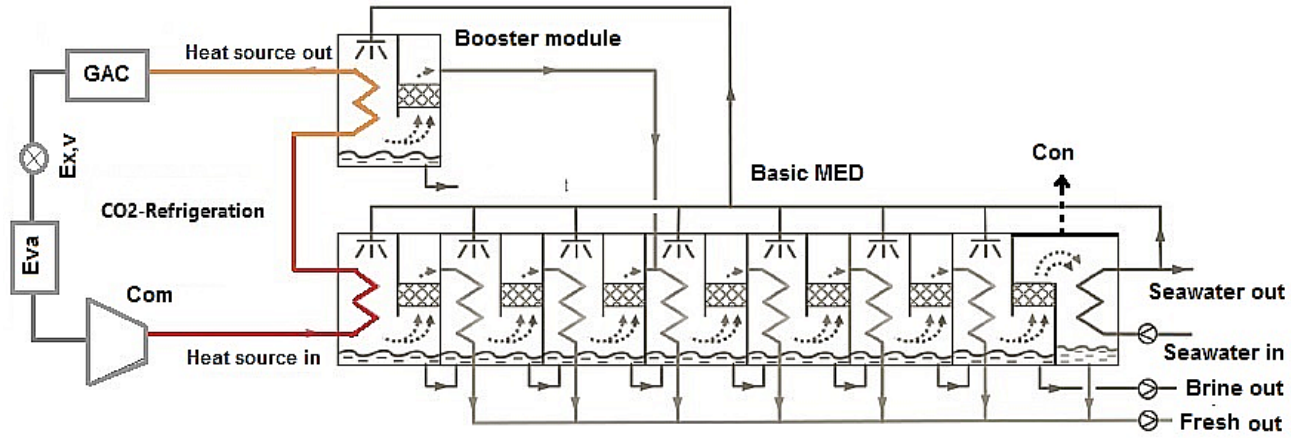

Fig. 1. Schematic diagram of the combined Boosted-MED system with transcritical carbon dioxide refrigeration system.

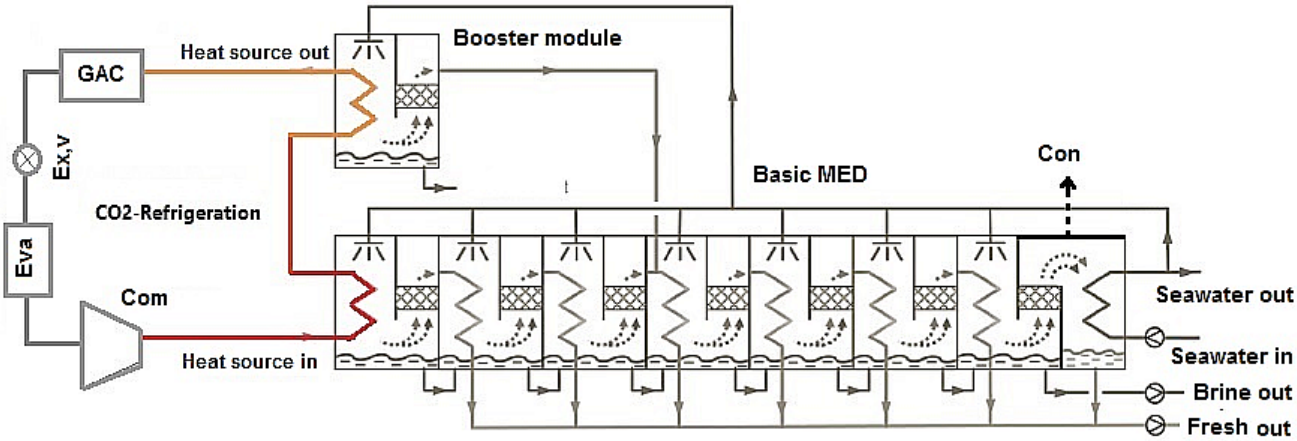

Fig. 1. Schematic diagram of the combined Boosted-MED system with transcritical carbon dioxide refrigeration system.

still has proper enough temperature (about 55–70°C) with the remarkable energy, it could be applied into the Booster module. Moreover, the other model is shown in Fig. 2, in which there are five water pre-heaters. The refrigerant leaves the MED's first stage, enters into the pre-heaters and rises up the sea water temperature and then comes into the gas cooler and passes through the rest of the refrigeration cycle. It should be mentioned that in this model, the applied equipment and length of piping are more than the boosted model, so there would be more losses and pressure drop associated with this model [7].

2.2. Modeling and assumptions

To simplify the thermodynamic analysis, the following assumptions are made regarding the two combined models:

Both two combined systems are operating at steady state condition.

- The environmental dead states of the system are chosen as the ambient temperature of 35°C, one atmospheric pressure, and the salinity of 46,500 ppm for seawater.
- The produced distillated water is assumed to be completely pure (w = 0 kg/kg) and the salinity of rejected brine is 70,000 ppm [17].
- The distillated water of each effect is a saturated liquid (x = 0).
- Minimum temperature differential (ΔT) between the following effects of MED is about 3°C [7, 8].
- The specific auxiliary power required in MED system assumed to be 1.2 kW per m^3 of produced fresh water [18].
- The gas-cooler temperature (T_5) is assumed 5°C higher than the ambient temperature.
- The isentropic efficiency of the carbon dioxide compressor is determined by the following equation [19].

$$\eta_{isen} = \begin{cases} -0.1234PR^4 + 1.1251PR^3 - 3.8902PR^2 + 6.0433PR - 2.8860 \; for \; PR < 2.7 \\ -0.0237PR^4 + 0.3051PR^3 - 1.474PR^2 + 3.1348PR - 1.7978 \; for \; PR \geq 2.7 \end{cases} \quad (1)$$

where PR is the pressure ratio

- The cooling demand of CO_2 refrigeration system is typically 200 kW.
- The electrical and mechanical efficiencies of the compressor are 90% and 85% respectively, and the pump efficiency in MED assumes to be 85%.

2.3. Thermodynamic analysis

The energy equations of transcritical CO_2 refrigeration and Boosted-MED are found in the literature [6] and for MED-PH, the detailed correlations are brought in the following section. As well as, the energy efficiency, the amount of desalinated water and COP of the refrigeration system are estimated through the energy analysis. The equations of thermodynamic analysis can be summarized into the conservation of mass, energy and exergy. The overall mass and energy balance equations for steady state conditions are:

$$\sum_{in} \dot{m}_{in} - \sum_{out} \dot{m}_{out} = 0 \tag{2}$$

$$\dot{Q} - \dot{W} = \sum_{in} (\dot{m} \times h) - \sum_{out} (\dot{m} \times h) \tag{3}$$

The salinity balance equations for the first effect and effect are given by Eqs. (4) and (5), respectively.

$$w_{sw} \cdot \dot{m}_{f1} = w_{Br,1} \cdot (\dot{m}_{f1} - D_1) \tag{4}$$

$$w_{sw} \cdot \dot{m}_{f1} + w_{Br(i-1)} \cdot \dot{m}_{Br(i-1)} = w_{Br(i)} \cdot \dot{m}_{Br(i)} \tag{5}$$

where w, Br and D_1 are salinity, brine stream and distilled water production rate in the first effect, respectively.

Since the pressure drop phenomenon in CO_2 transcritical refrigeration affects the thermodynamic properties of CO_2 in the refrigeration cycle, the pressure drop per length is calculated by following equation:

$$dp(KPa/m) = 0.001 \cdot f \cdot \frac{1}{2} \cdot \frac{1}{D_i} \cdot \rho \cdot u^2 \tag{6}$$

in which f, D_i, ρ and u are fraction factor, tube inner diameter (assumed to be 7.5 mm), density and velocity of bulk flow [20,21].

2.3.1. MED-PHs

The mass, salinity and energy balance equations for the first effect, effects 2 to n, condenser and pumps in MED-PHs are similar to Booted-MED.

2.3.1.1. Pre-heaters

At high heat source temperature, the effectiveness of pre-heaters are chosen which they reach the feed water to its corresponding boiling point. Correlation of energy balance for water pre-heaters is given by:

$$\dot{Q}_{PH_i} = \dot{m}_{co2} \cdot (h_{3,i(in)co2} - h_{3,i(out)co2}) = \dot{m}_{fi} cp_w (T_f - T_{f'}) \tag{7}$$

where $T_{f'}$ is the outlet temperature of seawater, leaving from the corresponded pre-heater. The effectiveness of pre-heaters determined by Eq. (8), [24].

$$\frac{\dot{Q}_{PH}}{\dot{Q}_{\max}} = \varepsilon \tag{8}$$

in which $\dot{Q}_{\max}$ can be obtained by Eqs. (9) and (10), [24].

$$\dot{Q}_{\max} = Cp_{\min} \times (T_{co2i} - T_f) \tag{9}$$

$$Cp_{\min} = \min(cp_w \times \dot{m}_f, cp_{co2} \times \dot{m}_{co2}) \tag{10}$$

2.3.2. COP and recovery ratio (η)

The COP of the transcritical CO_2 refrigeration system and the recovery ratio of MED are given by Eqs. (11) and (12), respectively.

$$COP = \frac{\dot{Q}_{eva}}{\dot{W}_{com}} \tag{11}$$

$$\eta(\%) = \frac{D_t}{\dot{m}_f} \times 100 \tag{12}$$

where D_t is the total fresh water production rate.

2.3. Exergy analysis methodology

Exergy is the maximum capacity of a system to do work, so the system reaches to the equilibrium with environment from the initial state. Exergy analysis is used to achieve the thermodynamic behavior of system at the time of energy conversion. Second law efficiency is a very effective parameter to evaluate an actual thermodynamic performance and processes [25–27]. In general, exergy is divided into two categories: maximum physical exergy, and chemical exergy. Physical exergy is the maximum value of the work that a system can produce, and this occurs when the system reaches to the mechanical (pressure) and thermal equilibrium with its surroundings. In fact the temperature and pressure of the system reaches to the temperature and pressure of the environment (dead state), while the concentration of the system does not change. On the other hand, chemical exergy is related to the concentration changes of a system from its initial value to the reference environment level in which the pressure and temperature remain constant [26,27]. The general form of exergy balance equation for a steady state system is as follows [27].

$$\sum_j \left(1 - \frac{T0}{Tj}\right) \times \dot{Q}_j - \dot{W}_{cv} \sum_{in} (\dot{m} \times e) + \sum_{out} (\dot{m} \times e) = \dot{E}_D \tag{13}$$

where $\dot{E}_D$ the exergy destruction and e is the specific exergy rate which is calculated by Eq. (14), [26–29].

$$e = (h - h^*) - T0 \times (s - s^*) + \sum_i w_i \times (\mu_i^* - \mu_i^0) \tag{14}$$

in which w and μ are mass fraction and chemical potential, respectively. These parameters can be calculated by correlations from references [26–32], which are presented in Appendixe A. Subscript i stands for the number of substance in the system. Superscript '0' represents ambient conditions (pressure, temperature and concentration), while superscript '*' refers to ambient pressure and temperature and the initial concentration of the system conditions.

The last section of Eq. (14) (chemical exergy) must be considered for the seawater. Ignoring it may lead to unrealistic and unreasonable results for the exergy variation with the concentration. Meanwhile, considering the fact that the carbon dioxide concentration does not change in the refrigeration cycle, the last term of Eq. (14) would be omitted in the exergy analysis of this cycle.

In second law efficiency explanation, the useful exergy output of the system must be correctly explained. In this study, the gained exergy is defined as the sum of the exergy of the cooling demand and the distilled produced water. As well as,the supplied exergy is the total power consumption of the system plus the exergy of the seawater entering the control volume. Therefore, in this combined system the second law efficiency is defined as follows:

$$\eta_{ex} = \frac{\left(\left|1-\frac{T_0}{T_L}\right|\right)\times \dot{Q}_{eva} + \sum_i \left(D_i \times e_{Di}\right)}{\dot{E}_{supply}} = 1 - \frac{\dot{E}_D}{\dot{E}_{supply}} \tag{15}$$

$$\dot{E}_{supply} = \dot{W}_{elec} + \left[\left(\dot{m}_f + \dot{m}_{cw}\right)\times e_{sw}\right] \tag{16}$$

$$\dot{W}_{elec} = \frac{\dot{W}_{com}}{\eta_{mec}\times\eta_{elec}} \tag{17}$$

where exergy destruction ($\dot{E}_D$) represents lost available work due to irreversibility within the system and discarding streams to the environment that carry exergy [27,28]. The supplied exergy in single generation systems is determined by:

$$\dot{E}_{supply,single} = \dot{W}_{elec} + \left[\left(\dot{m}_f + \dot{m}_{cw}\right)\times e_{sw}\right] + \dot{W}_{pumps} + \left(\dot{E}_{in,MED} - \dot{E}_{out,MED}\right) \tag{18}$$

$$\eta_{ex} = \max \tag{19}$$

Here, to solve the present optimization problem, the Genetic Algorithm (GA) is used. GA is an efficient search technique employed in computing to find exact or approximate solutions to optimization. In GA, an applicant solution to a problem is called a chromosome, and the evolutionary viability of each chromosome is determined by a fitness function. This method is a powerful optimization tool for nonlinear problems [25]. In this case-study to discover the efficient operating condition in the dual-generation system in which adequate fresh water production and high performance of refrigeration cycle occur simultaneously, the second law efficiency has been maximized. The parameters applied in GA for optimization of the system is presented in Table 1. The decision variables; evaporator temperature (T_{eva}), ambient temperature (T_{amb}), compressor output pressure (P_{comb}) and MED's first effect temperature (*TBT*) in output parameters is presented at following.

Table 1
Setting parameters in GA algorithm

Number of population	800
Crossover percentage	0.9
Mutation percentage	0.3
Number of generation	1400
Mutation rate	0.02

2.4. Simulation tool

Due to the complexity of the system analysis, that includes several control flows and volumes, EES [39] software has been used to solve the equations. The simulation is carried out according to the specified thermodynamic properties for different working fluids (CO_2 in refrigeration system; brine, steam and pure water in MED). Although most of the current models uses an iterative common method in a sequential numerical package such as MATLAB, a benefit of using an equation solver (EES) is that the programmer does not need to develop algorithms for solution convergence. The governing equations in equation solver are inputted, and then the solver recognizes and classifies the equations that should be solved for the system iteratively.

2.5. Solution verification

The simulated model was validated with those found in the relevant literature [6], from the energy aspect at the same operating conditions. For the exergy view point, the supercritical CO_2 refrigeration is verified with Shariatzade et al. [14]. Fig. 4 shows the change of second law efficiency graph of the current work and the one presented by [14]. It indicates that there is a good agreement between the results acquired from the present simulation and those reported in literature, with a maximum diversity of 3.8%.

3. Results and discussion

Since the main parameters such as evaporator temperature (T_{eva}), ambient temperature (T_{amb}), compressor output pressure (P_{comb}) and MED's first effect temperature (*TBT*) have the most effects on the system performance, these parameters have been investigated in this research. Effects of these parameters on COP and recovery ratio (η (%)), have been studied by energy analysis. Moreover, in a more detailed analysis and in

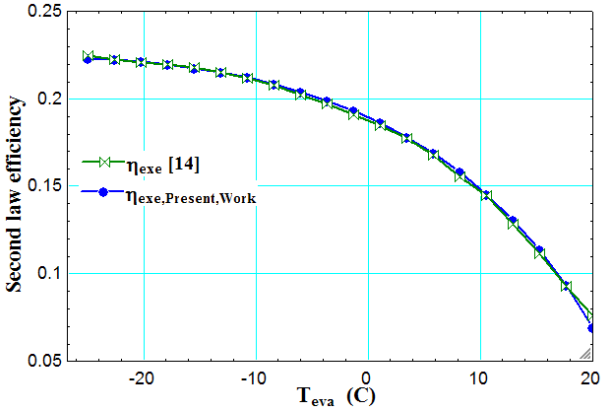

Fig. 3. Comparison of the exergy efficiency vs. evaporator temperature of the present simulation with those reported by Joneydishariatzadeh [14]. (T_{amb} = 40°C, P_{com} = 10270 KPa).

order to determine the amount of irreversiblities, exergy analysis has been performed. Exergy analysis reveals the quality of energy consumption, the amount of exergy loss in each component of system and the changes of second law efficiency in different working conditions. In addition, a comparison of two different models of water desalination systems; MED-PHs and Boosted-MED has been conducted.

3.1. Effect of evaporator temperature (T_{eva})

Fig. 4 shows the changes of COP and recovery ratio (η) against the evaporator temperature. For a specific amount of cooling capacity ($\dot{Q}_{eva} = 200kW$) with a reduction in the evaporator temperature, the compressor power consumption will increase. Therefore, the COP of refrigeration system reduces which results in the increment of heat loss from the refrigeration system. On the other hand, as a part of this heat loss is recovered by the MED system, the more fresh water would be produced and consequently the recovery ratio increases. Since the salt deposition in evaporator pipes causes adverse effect on the heat transfer process, the concentration of brine from the desalination system should not exceed of a specific value. So, the feed flow rate should be increased along with the reduction of evaporator temperature at the same time. At the lower evaporator temperatures (–40°C to –15°C), the both MED models (Boosted and PHs) produce almost the same amount of fresh water. With an increase in the evaporator temperature (lower heat source temperature for MED), the PHs is considerably less effective than the Boosted model. This is mainly due to the incapable of pre-heaters to increase the feed seawater temperature to their relative effects. As this constraint does not apply to the Booster module, a superior usage of the low-grade heat can be extracted at low temperatures, causing an increase in the distillated water production.

Considering Fig. 4 reveals the insufficiency of the energy study in multi-generation system analysis, in which the changes of COP and recovery ratio are in a contrary way. So, in order to have a better insight of the system overall performance, a parameter should be used to include both the effects of the cooling demand and the fresh water. This parameter is the second law efficiency and Fig. 5 shows the change of second law efficiency in the combined system with respect to the changes in the evaporator temperature. According to Eqs. (15) and (16), many parameters, such as the reference temperature (T_0), the cooling capacity (T_{eva}), the amount of fresh water production and the compressor power consumption are associated with the definition of exergy efficiency. At the constant cooling capacity and reference temperature, the increase in the evaporator temperature results in a decrease in the fresh water production rate, as well as compressor the power consumption. So, there is an optimum evaporator temperature (about –10°C) at which the both subsystems have their optimum performance and consequently the exergy efficiency is maximum.

With an increase in the evaporator temperature, the second law efficiency of the combined system increases in most of the temperature range. The single generation system in this study is defined as the systems which include a CO_2 refrigeration system with 200 kW cooling capacity and an MED system consumes methane to produces the same amount of fresh water. As can be seen, the exergy efficiency of the CO_2 refrigeration-MED (both PHs and Booster module) is considerably higher than that of a single generation system. It is because that the exergy lost in the single generation systems that it is recovered to a large extent in the combined system. It is observed in Fig. 5 that for the boosted model, the second law efficiency enhances from 0.034 to 0.17 in single generation and dual generation, respectively at the optimum evaporator temperature (–10°C).

3.2. Effect of ambient temperature (T_{amb})

Fig. 6 presents the graphs of COP and recovery ratio against the ambient temperature. Fig. 8 indicates that at the high enough evaporator temperature (–2°C), the fresh water flow rate increases and the COP of the system decreases with an increase in the ambient temperature. In addition, when the ambient temperature raises, the performance of Boosted system would be better and it can produce more fresh water than MED-PHs. Fig. 7 shows the changes of the second law efficiency versus the changes of the ambient temperature. With the increase of ambient temperature, both the numerator and denominator of Eq. (15) increase with different rates and the parabolic graphs

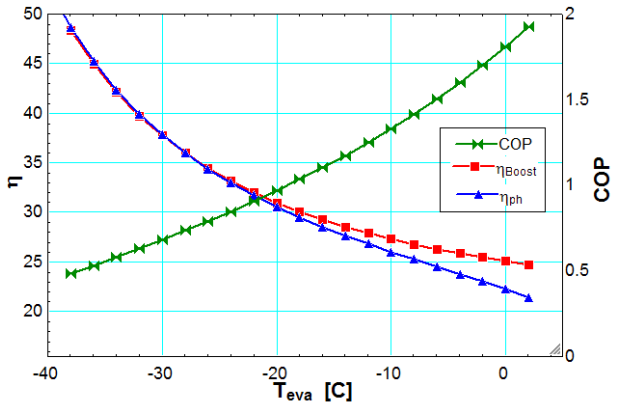

Fig. 4. Effect of the evaporator temperature on COP and Recovery ratio (η (%)). (T_{amb} = 35°C, P_{com} = 10570 kPa).

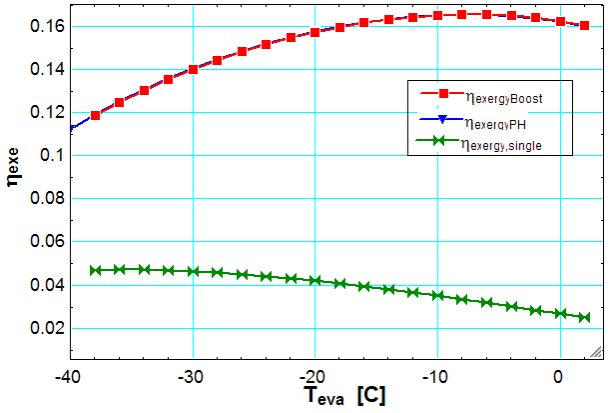

Fig. 5. Effect of the evaporator temperature on the second law efficiency at different MED configurations. (T_{amb} = 35°C, P_{com} = 10570 KPa).

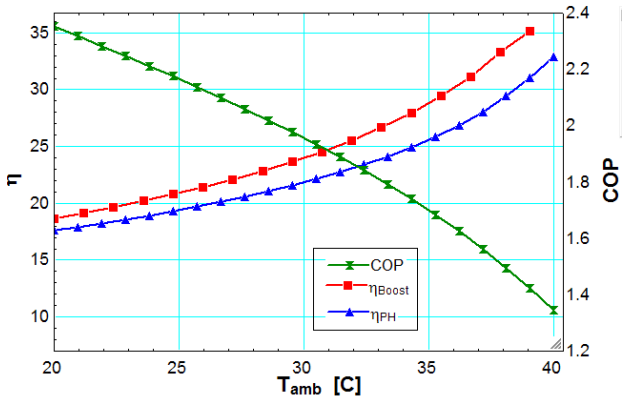

Fig. 6. Effect of the ambient temperature on COP and recovery ratio (η (%)). (T_{eva} = –2°C, P_{com} = 10570 kPa).

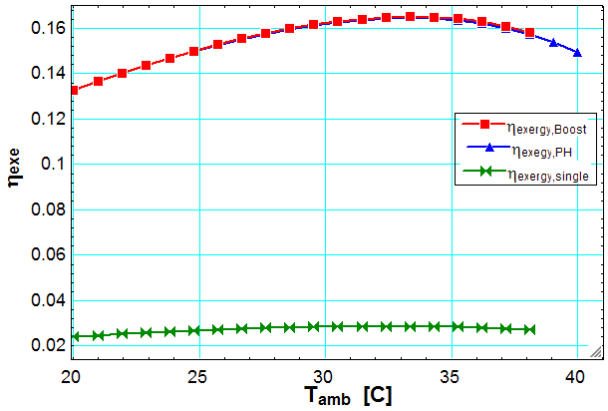

Fig. 7. Effect of the ambient temperature on second law efficiency. (T_{eva} = –2°C, P_{com} = 10570 kPa).

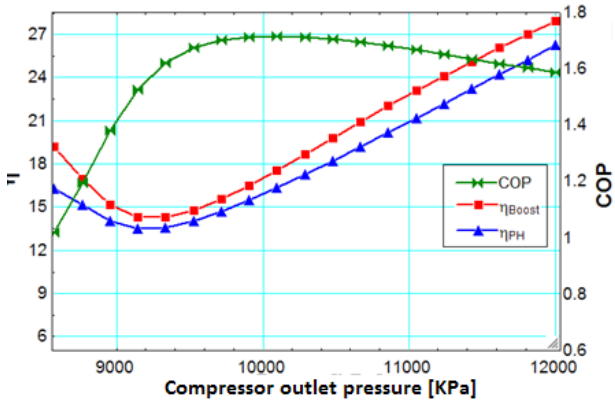

Fig. 8. Effect of the compressor outlet pressure on the COP and recovery ratio (η (%)). (T_{eva} = –2°C, T_{amb} = 35°C).

for the exergy efficiency has been created. Furthermore, the maximum point happens at about the optimum operating point of the system, and then there is a slight drop in exergy efficiency. Therefore, at the optimum ambient temperature (34°C) the exergy efficiency has its highest value. As can be

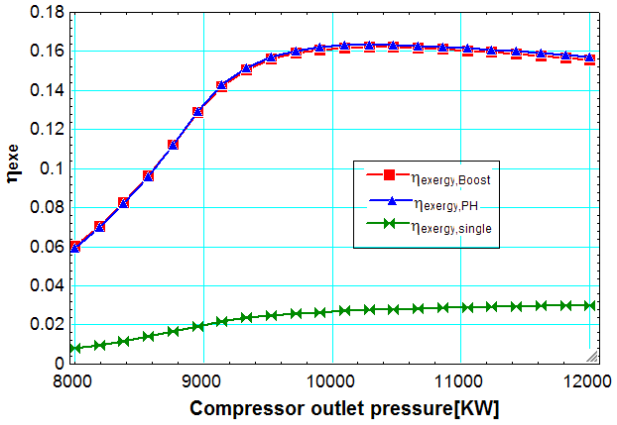

Fig. 9. Effect of the compressor outlet pressure on the second law efficiency. (T_{eva} = –2°C, T_{amb} = 35°C)

seen in Fig. 7, the exergy efficiency of MED-PHs is close to the boosted type, but due to use of pre-heaters before each stage, the amount of equipment and pressure drop in this system increase [7]. According to Fig. 7 for the combined Boosted and PHs systems, the exergy efficiency at the optimum ambient temperature (34°C) reaches the value of 0.171 and 0.17, respectively.

3.3. Effect of compressor output pressure (P_{com})

Fig. 8 represents the effect of compressor's output pressure on COP and recovery ratio. Fig. 8 reveals that at T_{eva} = –2°C and T_{amb} = 35°C, the optimum output pressure would be around 10,000 kPa. At this point, the compressor's power consumption is the least, which means that the highest COP is achieved. In order to produce a constant amount of refrigeration, with an increase in output pressure after the optimum point (highest COP), a tangible reduction of the CO_2 refrigerant flow rate happens. Consequently, the heat rejection to the environment reduces which means that the less heat would be available for the MED system. So, at the optimal output pressure of compressor, the system has the highest COP as well as the lowest amount of produced fresh water. Fig. 9 shows the effect of the compressor's outlet pressure on the second law efficiency of all the examined systems. As mentioned before, the compressor power consumption at its optimum pressure is the minimum. So, according to Eqs. (15) and (16), the second law efficiency at this point reaches its maximum. According to Fig. 8, after the optimum pressure point, COP reduces slightly but fresh water production increases sharply. Considering these two effects, the second law efficiency has no significant reduction after the optimum pressure point.

3.4. Exergy destruction

In order to have a better insight of the system, the exergy loss and its variations at different operating conditions have been studied for the following components (see Fig. 10).

- GAC1, is the gas cooler of the refrigeration system in single generation system.

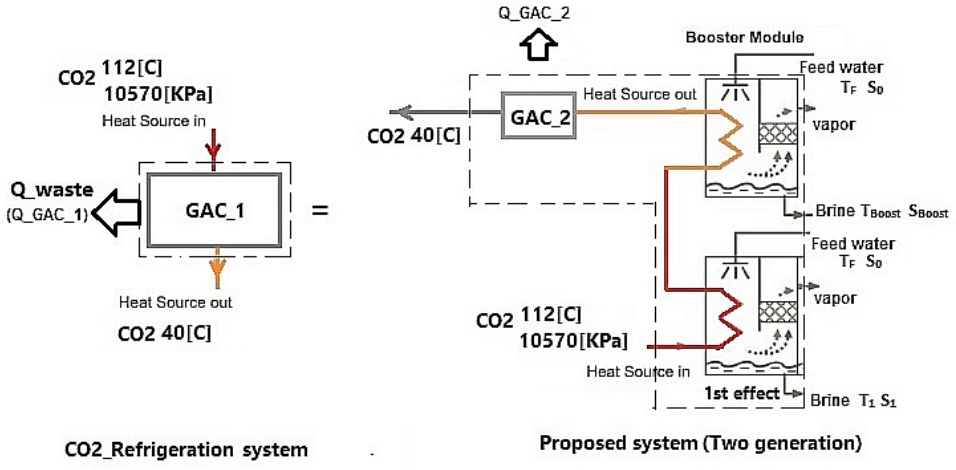

Fig. 10. Schematic diagram of the gas cooler of the CO_2 refrigeration (GAC1) in single generation and replaced parts included first effect, booster module and GAC2 in dual generation (substituted part).

- Substituted part which is the replaced system for GAC1, including first effect, booster module and gas cooler of the combined system (GAC2).

It should be noted that, since MED-Boosted has a better performance in combination with the sensible heat source, Figs. 11–13 are presented for this model. Figs. 11, 12 and 13 show the exergy destruction changes of GAC1 in the single refrigeration system and its replaced set (substituted part) against the evaporator temperature, ambient temperature and compressor outlet pressure, respectively. As can be seen in all three figures, the exergy destruction in GAC1 is far more than that of GAC2, even more than that of the whole replaced system (substituted part).

The reduction of evaporator temperature, as well as the increase of ambient temperature result in an increase of the CO_2 refrigerant temperature entering the MED's first effect. At the same time, the temperature of the refrigerant leaving the first effect does not considerably change. Although more fresh water is produced, but the difference between the exergy containment of the inlet and outlet streams of the MED's first effect increase. Therefore, the more exergy would be destructed in the first stage of the system. The same results can be found out when the compressor outlet pressure increases after its optimum value. As mentioned before, there is no considerable change in the refrigerant temperature entering the booster stage. On the other hand, the temperature of the refrigerant leaving the booster module does not undergo the significant changes either. Therefore, a major variation in lost exergy of this component cannot be seen through the changes of operating conditions. Moreover, the reduction of input temperature of CO_2 refrigeration to GAC2 results in a decrease in the destroyed exergy.

Tables 2 and 3 show the energy consumption, total exergy destruction rate and second law efficiency in different examined systems. The pinch point consideration is also an important study that should be taken into account for the steam generator heat exchanger designs. Pinch analysis for integration process are applied to maximize the process of heat recovery. For the heat exchanger design, the pinch

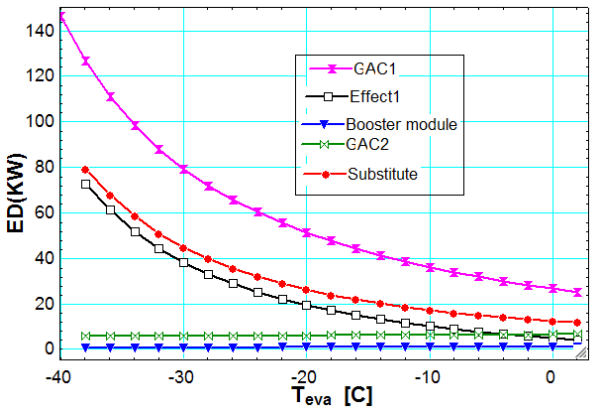

Fig. 11. Exergy destruction of the gas-cooler (single generation system) and its replacements (combined Boosted-MED system) at different evaporator temperatures. (T_{amb} = 35°C, P_{com} = 10570 KPa).

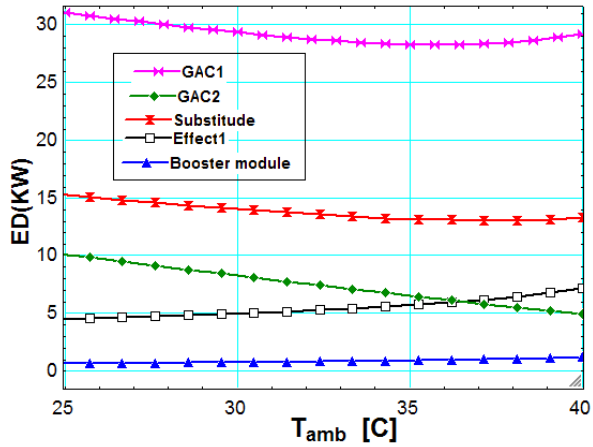

Fig. 12. Exergy destruction of the gas-cooler (single generation system) and its replacements (combined Boosted-MED system) at different ambient temperatures. (T_{eva} = –2°C, P_{com} = 10570 KPa).

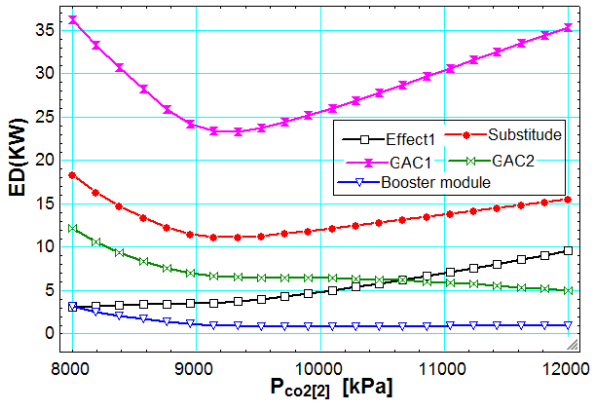

Fig. 13. Exergy destruction of the gas-cooler (single generation system) and its replacements (combined Boosted-MED system) at different compressor outlet pressures. (T_{eva} = –2°C, T_{amb} = 35°C).

Table 2
Comparison of the energy consumption and total exergy destruction for different systems (T_{eva} = –2°C, T_{amb} = 35°C, P_{com} = 10570 kPa)

System	Energy Consuming (kW)	Exergy destruction (kW)
CO_2-refrigeration	153.7	130.76
MED-boosted (RR = 28.8%)	120	44.362
MED-pHs (RR = 25.6%)	105	44.36
CO_2 Ref + MED- boosted (RR = 28.8%)	153.7	37.57
CO_2 Ref + MED- pHs (RR = 25.6%)	153.7	126.01

Table 3
Second law efficiency for different configuration (T_{eva} = –2°C, T_{amb} = 35°C, P_{com} = 10570 kPa)

Two generation system	Single generation system
Boosted(RR = 28.8%) : 16.33	Boosted(RR = 28.8%) : 3.14
PHs(RR = 25.6%) : 16.24	PHs(RR = 28.8%): 2.92
$\dot{Q}_{eva} = 200kW$	

point in the temperature profile of the evaporator has to be taking into account as the smallest temperature different between the heating medium and the partially evaporating feed. As it is shown in Fig. 17, the pinch point temperature ($T_{H,PP}$) is then used as a variable boundary condition to restrict the top brine temperature and the vapor temperature of the first effect and ΔT_{hex} is the lowest temperature different allowed at this location across each heat exchanger. It can be seen that the combined system; Boosted-MED-CO_2 Refrigeration, reduces the energy consumption of the system by 44% and decreases the total exergy destruction rate by 30.45%, compared the single generation system. The same parameters for the MED-PHs-CO_2 Refrigeration system are 40% and 25.14% respectively. According to Table 3, by integrating these two single generation systems, the second law efficiency enhances from 3.14% to 16.33% and 2.92% to 16.24% in boosted and pHs models respectively.

3.5. The influence of TBT

In addition to the evaporator temperature, ambient temperature and compressor outlet pressure, which play key roles in the system behavior, the top brine temperature (TBT) is also one of the influential parameters. Conventional MEDs are commonly optimized for being steam driven. Sensible heat sources in contrast require specific approaches to reveal their potential. As mentioned before, in a MED with sensible heat sources, TBT is compelled by the gradient of temperature drop in order to extract energy, rather than heat source input temperature.

Fig. 15 shows the changes of the exergy destruction in the first stage, booster, and gas cooler of the system in terms of TBT. Under constant temperature of CO_2 refrigerant entering to the first effect, by reducing the TBT, as the temperature differential between the effects drops down until the allowable value, the refrigerant outlet temperature reduces. Therefore, more fresh water would be produced and the difference between the exergy of the inlet and outlet streams increases. So, the exergy destruction of the first stage and consequently, the booster stage, increase. On the other hand, because of the reduction in the refrigerant temperature entering the gas cooler, the exergy dissipation in this component considerably reduces. So in general, the exergy dissipation of the whole replaced system reduces.

Fig. 16 shows the effect of TBT on the second law efficiency and the recovery ratio for both of the proposed combined systems, under the same inlet conditions. As stated before, reducing TBT leads to an increase in the fresh water flow rate and a decrease in the dissipated exergy at the replaced system. So, in contrast to the other parameters in which the exergy efficiency is maximum at a specific parameter value, in the case of TBT, the second law efficiency increases consistently.

3.6. CO_2 emission

In conventional MED system which uses boiler to provide hot steam as latent heat source, the significant quantity of CO_2 will be established. The detailed components of boiler is depicted in Fig. 14. The combustion equation for the methane natural gas and the CO_2 emission are determined by the following equations [23,34]:

$$\lambda CH_4 + 0.756N_2 + 0.000345CO_2 + 0.0303H_2O \rightarrow y_{N_2}N_2 + y_{O_2}O_2 + y_{CO_2}CO_2 + y_{H_2O}H_2O \quad (20)$$

$$\lambda_{st} = \frac{m_{fuel}}{m_{oxidant}} \quad (21)$$

$$\dot{m}_{fu} = 16.043n \quad (22)$$

$$\dot{m}_{co2} = 44.01n \quad (23)$$

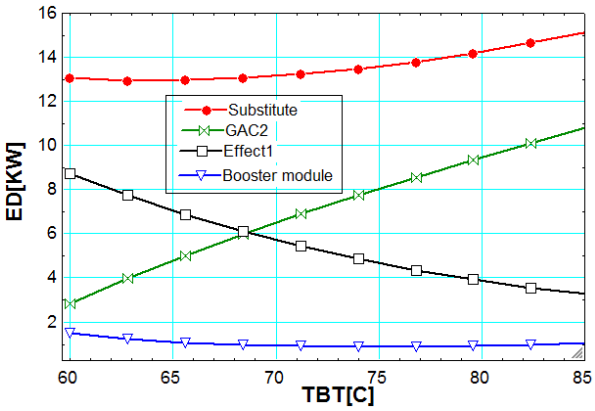

Fig. 14. Exergy destruction rate for the essential parts of the combined Boosted-MED system versus TBT. (T_{eva} = –2°C, T_{amb} = 35°C, P_{com} = 10570 KPa).

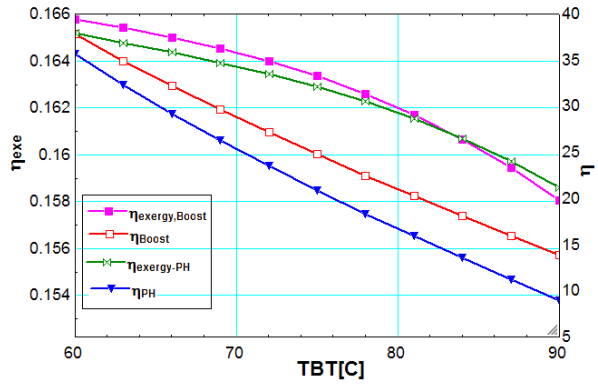

Fig. 15. Effect of TBT on the recovery ratio (η (%)) and second law efficiency for combined Boosted-MED and MED-PHs systems. (T_{eva} = –2°C, T_{amb} = 35°C, P_{com} = 10570 KPa).

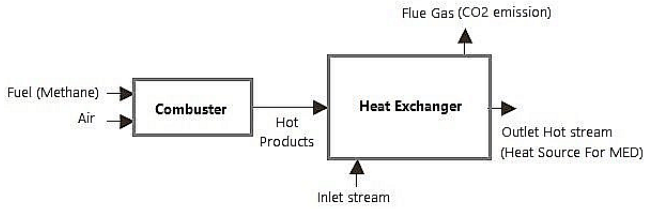

Fig. 16. Schematic diagram of a boiler.

Where λ and *n* are the fuel–oxidant ratio definition for the stoichiometric condition and the number of methane mole in the chemical reaction. Some assumptions like the complete consumption, negligible pressure loss in the boiler and steady state condition is considered in methane/air combustion. Since, the lower heating value of the methane is equal to 802.3 kJ/mol [34], according to Tables 2 and 3, and by attending to Eqs. (19) and (20), the annual CO_2 emission of the conventional MED for RR = 28.8% and RR = 25.6% are about 3403.84 and 2912.8 tons, respectively. So the combination of MED with transcriticalCO_2refrigeration can reduces considerably the environmental negative impacts.

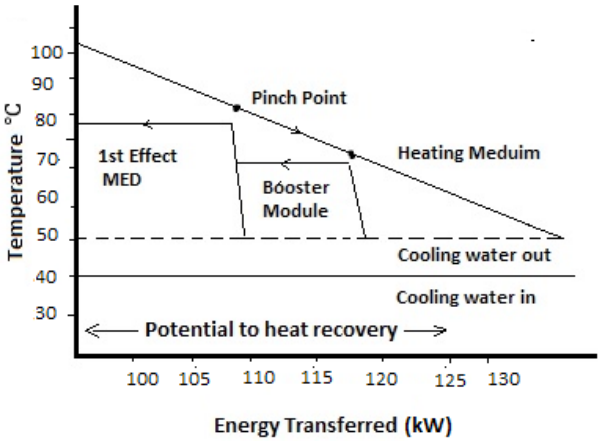

Fig. 17. Temperature profile of the Booster module and first effect of a MED vs. that of the sensible heat source in pinch analysis.

3 7. Sensitive analysis

A sensitivity analysis has been carried out in order to clarify the effect of some key parameters in the system responses. These responses are recovery ratio, COP and second law efficiency of the boosted-MED-CO_2 refrigeration system. The key parameters are consisting of the evaporator temperature, ambient temperature, compressor outlet pressure and TBT. From this analysis it would be possible to determine the effect of each parameter on the performance of the system.

By fitting a polynomial equation provided in Table 4, the connection between each response and parameter could be modeled to define the importance of the parameters' effects on the system responses. Also, the appropriation of the fit of the models examined by the coefficient of multiple correlation (R^2), which is presented in Table 4.

The derivation of the polynomial equation used to estimate the slope of the polynomial equation is presented for each response (in Table 5). Since the values of the slope of the polynomial equations changes with the variation of the parameter's values, by maximizing the derivative of the polynomial equation function in a parameter's domain, the sensitivity of each response with regard to that parameter is expressed by the maximum slope of the polynomial equation. It should be noted that in Table 4, in order to have the precise fit of the models, the multiple correlation coefficients values are selected so near to one (about 0.99).

The sensitivity values for COP, recovery ratio and second law efficiency, are shown in Figs. 18 a–c, respectively. According to Fig. 18a, for COP, the parameters of compressor output pressure, the ambient temperature and evaporating temperature are the lowermost effective parameters, respectively. The sensitivity values of the compressor output pressure and evaporating temperature are positive, which indicates that the influence of them on COP is additive. On the other hand, the negative value of the ambient temperature's sensitivity, expresses the reductive effect on the COP.

With respect to Fig. 18b, the ambient temperature has the highest sensitivity value with additive effect on the recovery ratio, which shows the ambient temperature importance on the fresh water production rate. After that, the TBT has the highest and reductive effect on recovery

Table 4
Polynomial equations for responses; COP, recovery ratio and exergy efficiency with respects to operating parameters

Polynomial equations	R^2
$COP(P_{com}) = 8E-10.P_{com}^{\ 3} - 3E-5.P_{com}^{\ 2} + 0.028.P_{com} - 99.34$	$R^2 = 0.986$
$COP(T_{eva}) = 0.9E-4.T_{eva}^{\ 2} + 0.0521.T_{eva} + 1.8423$	$R^2 = 0.997$
$COP(T_{amb}) = -1.3E-4.T_{amb}^{\ 2} - 1.89E-3.T_{amb} + 2.423$	$R^2 = 0.998$
$RR(P_{com}) = -2E-9.P_{com}^{\ 3} + 5E-4.P_{com}^{\ 2} - 0.516.P_{com} + 1805.1$	$R^2 = 0.99$
$RR(T_{eva}) = -8E-4.T_{eva}^{\ 3} - 1.7E-2.T_{eva}^{\ 2} - 0.433.T_{eva} + 14.657$	$R^2 = 0.998$
$RR(T_{amb}) = 2.66E-3.T_{amb}^{\ 2} - 1.731E-2.T_{amb} + 30.793$	$R^2 = 0.995$
$RR(TBT) = -1.74E-3.TBT^2 - 1.507.TBT + 110.41$	$R^2 = 0.999$
$eta_{exe}(P_{com}) = 7E-11.P_{com}^{\ 3} - 2E-6.P_{com}^{\ 2} + 0.023.P_{com} - 8.24$	$R^2 = 0.998$
$eta_{exe}(T_{eva}) = -0.83E-5.T_{eva}^{\ 2} - 6E-5.T_{eva} + 0.1639$	$R^2 = 0.998$
$eta_{exe}(T_{amb}) = -1E-5T_{amb}^{\ 3} + 0.6E-3.T_{amb}^{\ 2} - 0.91.T_{amb} + 0.139$	$R^2 = 0.995$
$eta_{exe}(TBT) = -0.1E-5.TBT^2 + 8.4E-3.TBT - 0.068$	$R^2 = 0.998$

ratio. In Contrast to the COP, in which the compressor outlet pressure is the most influential parameter, for the recovery ratio it has the minimum sensitivity value with a reductive effect. Finally, according to Fig. 18c, the sensitivity value for the second law efficiency is shown. The compressor output pressure and TBT has the highest and lowest values of sensitivity, with reductive and additive effects, respectively. So, it can be inferred that the compressor output pressure is the most important parameter in performance of the boosted-MED-CO_2 refrigeration system.

3.8. Using an expander in the presented combined system

Table 6 shows the exergy destruction of all components of the two combined systems in a given operating condition. Among the consecutive effects of MED, exergy destruction of the first effect and the booster module is more than the other effects. This is mainly because of the heat transfer process between the heat source and these two effects. The streams entering and leaving these heat exchangers contain considerable amounts of availability. So, the exergy destruction of first effect and booster module are more than other effects. As can be seen in Table 6, the maximum exergy destruction of the hybrid system happens in the compressor and expansion valve (ex. valve). Theoretical and practical examinations, such as two-stage compression [12] and application of expander [13], have been conducted in order to reduce the compressor power consumption. Although two-stage compression method reduces the power consumption of the compressor and improves the COP and second law efficiency (see Fig B.1), the amount of desalinated water reduces considerably because of the major reduction in the outlet temperatures of the compressors. On

Table 5
Derivative functions of polynomial equation with sensitivity values

Derivative function of polynomial equations	Sensitivity value
$\frac{dCOP}{dP_{com}} = 2.48E-9.P_{com}^{\ 2} - 6E-5.P_{com} + 0.028$	0.0004
$\frac{dCOP}{dT_{eva}} = 1.8E-4.T_{eva} + 0.0521$	0.00018
$\frac{dCOP}{dT_{amb}} = -2.6E-4 + 0.0189$	−0.00026
$\frac{dRR}{dP_{com}} = -6E-9.P_{com}^{\ 2} + 1E-3.P_{com} - 0.516$	−0.00277
$\frac{dRR}{dT_{eva}} = -2.4E-3.T_{eva}^{\ 2} - 3.4E-2.T_{eva} - 0.433$	−0.0034
$\frac{dRR}{dT_{amb}} = 5.32E-3.T_{amb} - 1.731E-2$	0.00532
$\frac{dRR}{dTBT} = -3.48E-3.TBT - 1.507$	−0.00348
$\frac{d(eta_{exe})}{dP_{com}} = 2.1E-10.?P_{com}^{\ 2} - 4E-6.P_{com}0.023$	0.000041
$\frac{d(eta_{exe})}{dT_{eva}} = -0.166E-4.T_{eva} - 6E-5$	0.0000166
$\frac{d(eta_{exe})}{dT_{amb}} = -3E-5T_{amb}^{\ 2} + 1.2E-3.T_{amb} - 0.91$	−0.0000094
$\frac{d(eta_{exe})}{dTBT} = -0.2E-5.TBT + 8.4E-3$	−0.000002

the other hand, according to Table 6, the exergy destruction of the ex. valve is also notable. Thus, the strategy of using an expander instead of the ex. valve in the combined system can provide the following advantages. Expander can produce a part of the power required for the compressor. It has also less exergy destruction than the ex. valve. Moreover, it has no effect on the refrigerant temperature leaving the compressor, so the fresh water flow rate will not reduce. In addition, Table 7 provides a comparison between three methods:

Method 1: One-stage compression using ex. valve
Method 2: two-stage compression using ex. valve
Method 3: One-stage compression using expander

With respect to Table 7, method 3 has the highest COP and second law efficiency, but a slightly lower recovery ratio compared to method 1. Fig. 19 shows the lost exergy of the various components in these three methods. As shown in Table 5, the COP and second law efficiency increase 22.2%

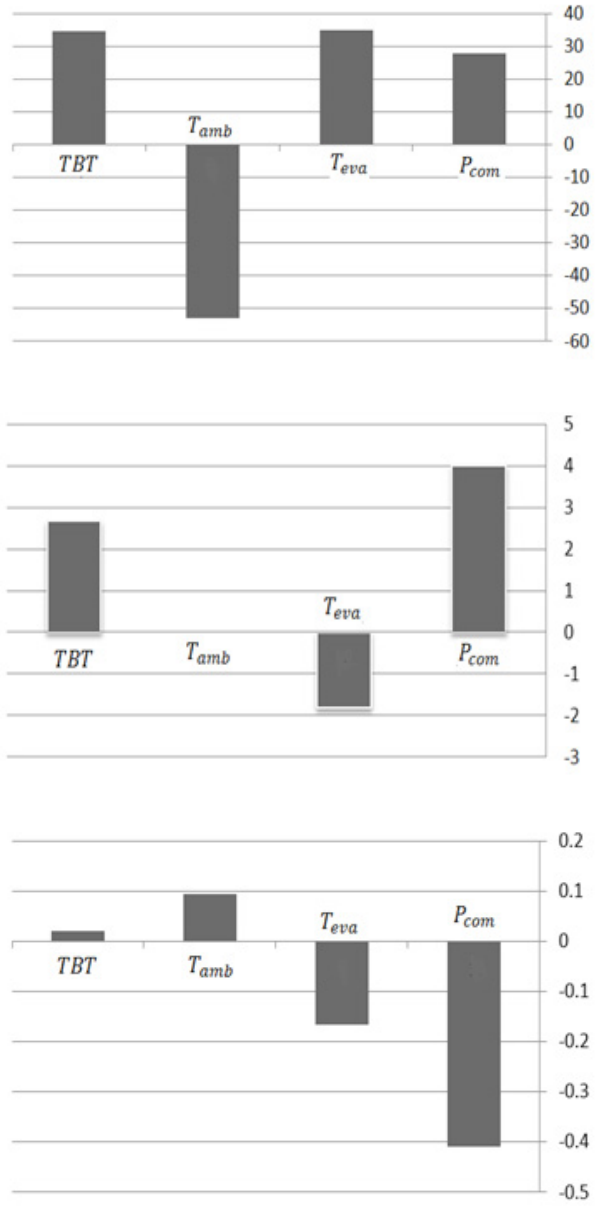

Fig. 18. Sensitivity values (×10⁴) for the Boosted-MED-CO_2Refrigeration system parameters: (a) recovery ratio (b) COP (c) second law efficiency.

and 18%, respectively, and the recovery ratio decreases only 2.8%, in method 3 compare to method 1. While, in method 2, the COP and exergy efficiency increase 5.1% and 2.9% respectively, and the recovery ratio decreases 32.7% compared to method 1.

It should be noted that in method 2, the first effect is considered as an inter-cooler, and the refrigerant leaves the second compressor with the same pressure of the single-stage compression system. Then the hot refrigerant enters the booster module of MED system. Moreover, the intermediate pressure is optimized, so the refrigeration system would reach the highest COP.

Table 6
Exergy destruction for different components of the combined MED-Boosted and MED-PHs systems (T_{eva} = –2°C, T_{amb} = 35°C, P_{com} = 10570 KPa)

MED Type		
System components	Boosted model	Pre-heaters model
Evaporator	4.42	4.42
Compressor	70.62	70.62
GAC_2	2.83	7.02
Ex. valve	27.52	27.56
Effect 1	5.7	5.17
Effect2	1.55	1.036
Effect 3	1.325	1.129
Effect 4	1.139	1.211
Effect 5	1.01	1.325
Effect 6	1.348	1.325
Booster module	2.9	–
Pre-heaters(n = 5)	–	2.43
MED-condenser	3.95	2.24
Pumps	0.37	0.38
ED_{Total}	121.78	126.01
ED_{GAC} stand-alone CO_2 refrigeration(GAC_1) = 28.2 kJ/kg		

T_{amb} = 35°C, P_{amb} = 10352 KPa, S_0 = 46.5 g/kg

Table 7
Comparison of COP, recovery ratio and second law efficiency in three methods

Parameter	Method		
	1:1Com +Ex.V	2:2com +Ex.V	3:1Com +Exp
COP	1.69	1.79	2.076
Recovery ratio (η) (%)	28.7	19.1	27.88
Second law efficiency	0.1638	0.1695	0.1932

T_{eva} = –2°C, T_{amb} = 35°C, $P_{out\ comp}$ = 10570 kPa

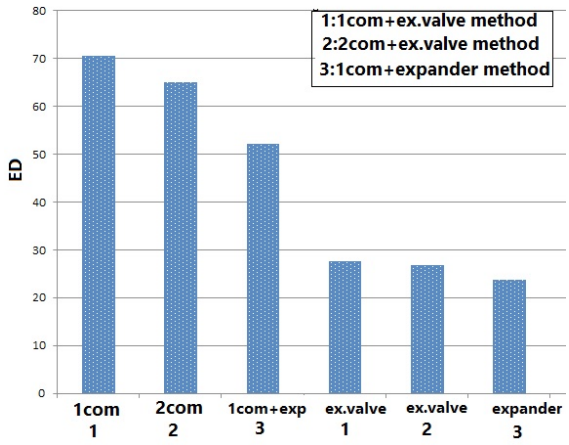

Fig. 19. Comparison of the exergy destruction in different parts for three methods.

4. Conclusion

A combination of transcritical CO_2 refrigeration system with two kinds of MED systems, Boosted-MED and MED-PHs, are studied and compared based on energetic and exegetic analyzes. The effect of some key parameters has been investigated on system performance. The results suggest that by variation of the evaporator and ambient temperature, the COP and recovery ratio change in a contrary way. So, the second law efficiency has a maximum value for a specific evaporator and ambient temperature. Moreover, in order to propose the best state of the hybrid system, genetic algorithm optimization is used. The significant upgrade in the combined system performance is associated to the exergy efficiency which increases up to 400% compared to the stand-alone system. On the other hand, Boosted-MED is able to produce more fresh water (14%) compared to MED-PHs. Furthermore, the following concluding notes are extracted from this study.

By increasing the compressor outlet pressure after the optimum point (highest exergy efficieny), the COP and second law efficiency reduce a little; 5.8% and 0.9%, respectively, while, the recovery ratio increases up to 86%. Therefore, the operation of proposed system after to its optimum pressure value could be suggested.

The decrease in the TBT results in an increase of the fresh water production, it increases the exergy destruction in first effect and Booster module, as well. But in general, the exergy dissipation of the whole replaced system reduces. Consequently, the second law efficiency increases consistently. Therefore, reducing TBT to a minimum allowable point at which the booster module still is effective, can upgrade the system performances.

The compressor and expansion valve are the most destructive components. So, by using the expander, in addition to enhances the second law efficiency (about 18%), there would be no effect on the compressor outlet temperature (in contrast to two-stage compression method). This causes that the fresh water production will not considerably decrease. Thus, regardless of economic considerations, replacing ex. valve with expander is recommended.

The sensitive analysis results showed that the compressor outlet pressure has the highest value of sensitivity on the COP and exergy efficiency, which indicates that it is the most effective parameter. On the other hand, the ambient temperature has the highest additive effect on the recovery ratio.

Symbols

BPE — Boiling point elevation (°C)
COP — Coefficient of performance
Cp — Specific heat (kJ/kg/K)
D — Distillate production rate (kg/s)
dp — Pressure drop per length (Kpa/m)
e — Specific exergy (kJ/kg)
EES — Equation engineering solver
$\dot{E}$ — Exergy rate (kW)
$\dot{E}_D$ — Exergy destruction rate (kW)
h — Specific enthalpy (kJ/kg)
h_{fg} — Latent heat (kJ/kg)
$\dot{m}$ — Mass flow rate (kg/s)
P — Pressure (KPa)
PH(*s*) — Pre-Heater (s)
$\dot{Q}$ — Net heat transfer rate (kW)
RR — Recovery Ratio (η (%))
s — Specific entropy (kJ/kgK)
T — Temperature (°C)
TBT — Top Brine Temperature (°C)
v — Specific volume (m^3/kg)
$\dot{W}$ — Net consumed power (kW)
w — Salinity (gr/kg)
x — Vapor quality

Subscripts

0 — Reference state
amb — Ambient
B — Booster
CO_2 — Carbon dioxide
com — Compressor
cw — Cooling water
cv — Controle volume
eva — Evaporator
elec — Electrical
Ex. value — Expansion valve
Exp — Expander
f — Feed seawater
GAC — Gas-Cooler
i — Effect number
in — Inlet
$\dot{m}$ — Mass flow rate (kg/s)
mec — Mechanical
out — Outlet
P_{com} — Compressor outlet pressure
Ref — Refrigeration
supply — Supplied to the system
sw — Seawater
vs — Vapor saturation
w — Water

Greek

ε — Heat exchanger effectiveness
η — Recovery ratio (%)
η_{ex} — Second law efficiency (exergy efficiency)
η_{mec} — Mechanical efficiency
η_{elec} — Electrical efficiency
μ — Chemical potential
Δt — Temperature differential over the effects (°C)

References

[1] W. Yongqing, N. Lior, Proposal and analysis of a high-efficiency combined desalination and refrigeration system based on the LiBr–H_2O absorption cycle—Part 1: System configuration and mathematical model. Energy Convers. Manag., 52(1) (2011) 220–227.
[2] T.P. Gregory, E.W. Tow, L.D. Banchik, H.W. Chung, J.H. Lienhard, Energy consumption in desalinating produced water from shale oil and gas extraction. Desalination, 366 (2015) 94–112.
[3] M.V.V. Rane, Y.S. Padiya, Heat pump operated freeze concentration system with tubular heat exchanger for seawater desalination, Energy Sustain Dev., 15 (2011) 184–191.
[4] S. Oumar, N. Galanis, M. Sorin, Thermodynamic study of multi-effect thermal vapour-compression desalination systems. Energy, 72 (2014) 69–79.

[5] V.G. Gude, N. Nirmalakhandan, Combined desalination and solar-assisted air-conditioning system, Energy Convers. Manag, 49(11) (2008) 3326–3330.
[6] A. Farsi, S.H. Mohammadi, M. Ameri, An efficient combination of transcritical CO_2 refrigeration and multi-effect desalination: Energy and economic analysis. Energy Convers. Manag, 127 (2016) 561–575.
[7] A. Christ, R.L. Klaus, C.T. Hui, Boosted multi-effect distillation for sensible low-grade heat sources: a comparison with feed pre-heating multi-effect distillation. Desalination, 366 (2015) 32–46.
[8] A. Christ, R.L. Klaus, C.T. Hui, Thermodynamic optimization of multi effect distillation driven by sensible heat sources. Desalination, 336 (2014) 160–167.
[9] M. Hosseini, I. Dincer, P. Ahmadi, H.B. Avval, M. Ziaasharhagh, Thermodynamic modelling of an integrated solid oxide fuel cell and micro gas turbine system for desalination purposes. Int. J. Energy Res., 37(5) (2013) 426–434.
[10] Y. Ma, L. Zhongyan, T. Hua, A review of transcritical carbon dioxide heat pump and refrigeration cycles, Energy 55 (2013) 156–172.
[11] Handbook, A. S. H. R. A. E. Refrigeration, 1791 Tullie Circle, NE Atlanta, GA 30329, 2010.
[12] J. Sarkar, A. Neeraj, Performance optimization of transcritical CO_2 cycle with parallel compression economization. Int. J. Therm. Sci., 49(5) (2010) 838–843.
[13] J.L. Yang, Y.T. Ma, M.X. Li, H.Q. Guan, Exergy analysis of transcritical carbon dioxide refrigeration cycle with an expander. Energy, 30(7) (2005) 1162–1175.
[14] O.J. Shariatzadeh, S.S. Abolhassani, M. Rahmani, M.Z. Nejad, Comparison of transcritical CO_2 refrigeration cycle with expander and throttling valve including/excluding internal heat exchanger: Exergy and energy points of view. Appl. Therm. Eng., 93 (2016) 779–787.
[15] J. Wang, P. Zhao, X. Niu, Y. Dai, Parametric analysis of a new combined cooling, heating and power system with transcritical CO_2 driven by solar energy. Appl. Energy, 94 (2012) 58–64.
[16] S.H. Mohammadi, M. Ameri, Energy and exergy analysis of absorption–compression hybrid air-conditioning system. HVAC & R Res., 19(6) (2013) 744–753.
[17] H.T. El-Dessouky, H.M. Ettouney, Fundamentals of Salt Water Desalination, Elsevier, 2002.
[18] L. Awerbuch, Understanding of thermal distillation desalination processes, IDA Academy, Singapore, 2012.
[19] A.H. Mosaffa, L.G. Farshi, C.I. Ferreira, M.A. Rosen, Exergoeconomic and environmental analyses of CO_2/NH_3 cascade refrigeration systems equipped with different types of flash tank inter coolers. Energy Convers. Manag., 117 (2016) 442–453.
[20] B.T. Austin, K. Sumathy, Transcritical carbon dioxide heat pump systems: A review, Renew Sust. Energ Rev., 15(8) (2011) 4013–4029.
[21] Z.B. Liu, Y.L. He, Y.F. Yang, J.Y. Fei, Experimental study on heat transfer and pressure drop of supercritical CO_2 cooled in a large tube. Appl. Therm. Eng., 70(1) (2014) 307–315.
[22] I.S. Al-Mutaz, I. Wazeer, Comparative performance evaluation of conventional multi-effect evaporation desalination processes, Appl. Therm. Eng., 73(1) (2014) 1194–1203.
[23] Y.A. Cengel, M.A. Boles, An engineering approach, Energy, 2002.
[24] R.K. Shah, D.P. Sekulic, Fundamentals of Heat Exchanger Design. John Wiley & Sons, 2003.
[25] I.J. Esfahani, A. Ataei, V. Shetty,T. Oh, J.H. Park, C. Yoo, Modeling and genetic algorithm-based multi-objective optimization of the MED-TVC desalination system, Desalination, 292 (2012) 87–104.
[26] M.H. Sharqawy, J.H. Lienhard, S.M. Zubair, Thermophysical properties of seawater: a review of existing correlations and data. Desal. Water Treat., 16 (2010) 354–380.
[27] H. Ghaebi, M. Amidpour, S. Karimkashi, O. Rezayan, Energy, exergy and thermo economic analysis of a combined cooling, heating and power (CCHP) system with gas turbine prime mover,Int. J. Energ. Res., 35(8) (2011) 697–709.
[28] A. Bejan, Advanced engineering thermodynamics, 3rd ed.; John Wiley & Sons, Inc: Hoboken, NJ, USA, 2006.
[29] M.J. Moran, Availability Analysis: A Guide to Efficient Energy Use. ASME Press, New York, 1989.
[30] J.R. Cooper, Release on the IAPWS Formulation 2008 for the Thermodynamic Properties of Seawater. The International Association for the Properties of Water and Steam, September, 2008, pp. 1–19.
[31] M.H. Sharqawy, J.H. Lienhard, S.M. Zubair, Formulation of seawater flow exergy using accurate thermodynamic data. International Mechanical Engineering Congress and Exposition, ASME, 5 (2010) 675–682.
[32] M.H. Sharqawy, S.M. Zubair, On exergy calculations of seawater with applications in desalination systems, Int. J. Therm. Sci., 50(2) (2011) 187–196.
[33] X. Wang, A. Christ, K. Regenauer-Lieb, K. Hooman, H.T. Chua, Low grade heat driven multi-effect distillation technology. Int. J. Heat Mass Transfer, 54 (2011) 5497–5503.
[34] J. Szargut, Exergy Method: Technical and Ecological Applications, 2005.
[35] Y.A. Çengel, M.A. Boles, Thermodynamics: an engineering approach, McGraw-Hill Education, 2015.
[36] H.T. El-Dessouky, H.M. Ettouney, F. Mandani, Performance of parallel feed multiple effect evaporation system for seawater desalination. Appl. Therm. Eng., 20(17) (2000) 1679–1706.

Appendixes

Appendix A. Correlations for Thermodynamic properties calculation:

A.1. Pure water enthalpy

The enthalpy of pure water states involving saturated water and saturated vapor can be calculated through Eqs. (A.1)–(A.15) [6] and [26,27].

A.1.1. The enthalpy of saturated water is calculated by Eq. (A.1) which is valid for 5 ≤ T ≤ 200°C [26–32]

$$h_w = 0.001.(141.355 + 4202.070 \cdot T - 0.535 \cdot T^2 + 0.004 \cdot T^3) \quad (A.1)$$

A.1.2. The enthalpy of saturated vapor can be calculated by Eq. (A.2) [35]

$$h_v = h_w + h_{fg} \quad (A.2)$$

A.1.3. h_{fg} is latent heat of evaporation calculated by (A.3) which is valid for 0 ≤ T ≤ 200°C [26–32]

$$h_{fg} = 0.001 \times (2.0501.10^6 - 2.369.10^3.T + 2.678.10^{-1}.T^2 - 8.103.10^3.T^3 - 2.079.10^{-5}.T^4) \quad (A.3)$$

A.2. Seawater

Correlations of seawater thermodynamic properties such as specific enthalpy, specific volume, specific entropy, and chemical potentials to be used in exergy analysis calculations are given.

A.2.1. Specific enthalpy

The enthalpy of seawater is calculated by (A.4), [26–32] which is valid for 0 ≤ w_s ≤ 0.12 kg/kg and 10 ≤ T ≤ 120°C:

$$h_{sw} = h_w - 0.001 \cdot w_s \cdot (b_1 + b_2 \cdot w_s + b_3 \cdot w_s^2 + b_4 \cdot w_s^3 + b_5 \cdot T + b_6 \cdot T^2 + b_7 \cdot T^3 + b_8 \cdot T \cdot w_s + b_9 \cdot w_s^2 \cdot T + b_{10} \cdot w_s \cdot T^2) \quad (A.4)$$

$$b_1 = -2.348 \cdot 10^4, b_2 = 3.152 \cdot 10^5, b_3 = 2.803 \cdot 10^6, b_4 = -1.446 \cdot 10^7, b_5 = 7.826 \cdot 10^3, b_6 = -4.417 \cdot 10^1$$

$$b_7 = 2.139 \cdot 10^{-1}, b_8 = -1.991 \cdot 10^4$$

$$b_9 = 2.778 \cdot 10^4, b_{10} = 9.728 \cdot 10^1$$

A.2.2. Specific volume

In order to take into account the effect of pressure in estimate of seawater enthalpy, Eq. (A.5) can be used to calculation the specific enthalpy of seawater at different pressures:

$$h_{sw}(T,P,w_s) = h_{sw}(T,P_0,w_s) + \nu.(P - P_0) \quad (A.5)$$

where $h_{sw}(T,P,w_s)$ is the specific enthalpy of seawater at atmospheric pressure calculated from Eq. (A.4) and v is the specific volume of seawater calculated from Eq. (A.6).

$$\nu = 1/\rho \quad (A.6)$$

$$\rho_{sw} = \rho_w + w_s \cdot (a_2 \cdot T + a_3 \cdot T^2 + a_4 \cdot T^3 + a_5 \cdot w_s \cdot T^2) \quad (A.7)$$

$$\rho_w = 9.999 \cdot 10^2 + 2.034 \cdot 10^{-2} T - 6.162 \cdot 10^{-3} \cdot T^2 + 2.261 \cdot 10^{-5} \cdot T^3 - 4.657 \cdot 10^{-8} \cdot T^4 \quad (A.8)$$

A.2.3. Specific entropy

The entropy of seawater is calculated by Eq. (A.9), (A.10), [26] which is valid for 0 ≤ w_s ≤ 0.12 kg/kg 10 ≤ T ≤ 120°C:

$$s_{sw} = s_w - 0.001 \cdot w_s \cdot (c_2 \cdot w_s + c_3 \cdot w_s^2 + c_4 \cdot w_s^3 + c_5 \cdot T + c_6 \cdot T^2 + c_7 \cdot T^3 + c_8 \cdot T \cdot w_s + c_9 \cdot w_s^2 \cdot T + c_{10} \cdot w_s \cdot T^2) \quad (A.9)$$

$$s_w = 0.001 \cdot (0.1543 + 15.383 \cdot T - 2.996 \cdot 10^{-2} \cdot T^2 + 8.193 \cdot 10^{-5} \cdot T^3 - 1.370 \cdot 10^{-7} \cdot T^4) \quad (A.10)$$

$$c_1 = -4.23 \cdot 10^2, c_2 = 1.463 \cdot 10^4, c_3 = -9.880 \cdot 10^4$$

$$c_4 = 3.095 \cdot 10^5, c_5 = 2.56 \cdot 10^1$$

A.2.4. Chemical potential

The chemical potentials of water in seawater and salts in seawater are resolute by differentiating the total Gibbs energy function with respect to the composition:

$$\mu_s = g_{sw} + (1 - w_s) \cdot \frac{\delta g_{sw}}{\delta w_s} \quad (A.11)$$

$$\mu_w = g_{sw} - (w_s) \cdot \frac{\delta g_{sw}}{\delta w_s} \quad (A.12)$$

where μ_s and μ_s are chemical potential of salts and water in seawater, and g_{sw} is the specific Gibbs energy of seawater calculated by Eq. (A.13).

$$g_{sw} = h_{sw,p} - (T_0 + 273.15) \cdot s_{sw} \quad (A.13)$$

where $h_{sw,p}$, and s_{sw} can be resoluted by Eqs. (A.5) and (A.9), respectively.

The differentiation of the specific Gibbs energy with respect to seawater salinity is determined by Eq. (A.14) [26]:

$$\frac{\delta g_{sw}}{\delta w_s} = \frac{\delta h_{sw}}{\delta w_s} - (T_0 + 273.15) \cdot \frac{\delta s_{sw}}{\delta w_s} \quad (A.14)$$

where $\frac{\delta h_{sw}}{\delta w_s}$ and $\frac{\delta s_{sw}}{\delta w_s}$ can be resoluted by differentiating the specific enthalpy and entropy of seawater with respect to sweater concentration as follows:

$$-\frac{\delta h_{sw}}{\delta w_s} = 0.001\cdot(b_1 + 2\cdot b_2\cdot w_s + 3\cdot b_3\cdot w_s^{\,2} + 4\cdot b_4\cdot w_s^{\,3} + b_5\cdot T_0 + b_6\cdot T_0^{\,2} + b_7\cdot T_0^{\,3} + 2\cdot b_8\cdot T_0\cdot w_s + 3\cdot b_9\cdot w_s^{\,2}\cdot T_0 + 2\cdot b_{10}\cdot w_s\cdot T_0^{\,2}) \quad \text{(A.15)}$$

$$-\frac{\delta s_{sw}}{\delta w_s} = 0.001\cdot(c_1 + 2\cdot c_2\cdot w_s + 3\cdot c_3\cdot w_s^{\,2} + 4\cdot c_4\cdot w_s^{\,3} + c_5\cdot T_0 + c_6\cdot T_0^{\,2} + c_7\cdot T_0^{\,3} + 2\cdot c_8\cdot T_0\cdot w_s + 3\cdot c_9\cdot w_s^{\,2}\cdot T_0 + 2\cdot c_{10}\cdot w_s\cdot T_0^{\,2}) \quad \text{(A.16)}$$

where *a* and *b* are acquired from Eqs. (A.8) and (A.8), respectively.

Appendix B. BPE in MED

The raise in the boiling temperature at a given pressure due to dissolved salts in the water is called the boiling point elevation (BPE). The following formula is used to calculate the BPE , [22,36].

$$BPE = AX + BX^2 + CX^3 \quad \text{(B.1)}$$

$$A = 8.325\times10^{-2} + 1.883\times10^{-4}\times T + 4.02\times10^{-6}\times T^2,$$

$$B = -7.625\times10^{-4} + 9.02\times10^{-5}\times T - 5.2\times10^{-7}\times T^2,$$

$$C = 1.522\times10^{-4} - 3\times10^{-6}\times T - 3\times10^{-8}\times T^2$$

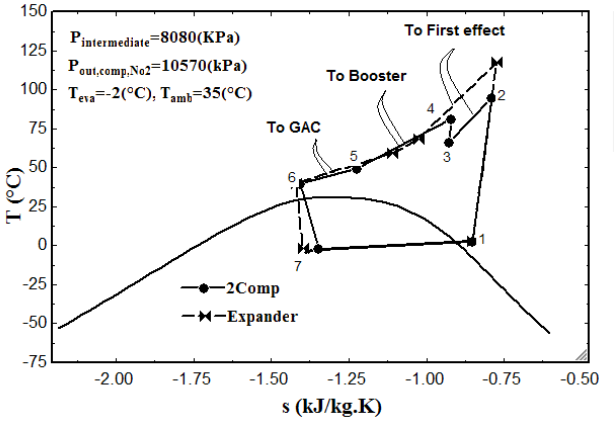

Fig B.1. T-S diagram of two improved methods; two-stage compression with ex. valve and one compression with expander.